Journal of Coastal Conservation (2022) 26:60
https://doi.org/10.1007/s11852-022-00907-x

Instability mechanisms and evolution of a rocky cliff on the Atlantic coast of Spain

Carlos López-Fernández[1] · María José Domínguez-Cuesta[1] · Pelayo González-Pumariega[2] · Daniel Ballesteros[3] · Lucas Suárez Suárez[1] · Montserrat Jiménez-Sánchez[1]

Received: 5 July 2022 / Revised: 2 November 2022 / Accepted: 3 November 2022 / Published online: 17 November 2022

Abstract
Predicting the response of rocky coasts to different erosional agents remains a great challenge at present. The episodic and discontinuous nature of the instability processes typical of hard bedrocks makes it difficult to make predictions based on observations over short research periods. This work aims to contribute to the understanding of the geomorphological evolution of rocky cliffs by means of a case study of a geologically complex cliff (developed on quartzite and slate) located on the Atlantic coast of Spain. The analysis of high-precision topographic models and orthophotographs, the use of geomatics techniques and geomorphological characterization have made it possible to define a model of the cliff behaviour. The results indicate that the structure of the bedrock determines the type of instability processes affecting the cliff and the morphology of the associated deposits. Lithology is the other main conditioning factor: while slate is easily eroded, quartzite offers greater strength and its detached blocks act as an effective natural defence element protecting the cliff and slowing down the coastal retreat. The evolution model established for this cliff explains the absence of retreat in the study period (2003–2022) and confirms the important role of local factors in cliff evolution.

Keywords Rocky coast · Cliff retreat · Mass movements · Slope deposits · Local factors · Atlantic coast

Introduction

Predicting the response of rocky coastal cliffs to different erosional agents remains a great challenge at present. The episodic and local nature of the instability processes characteristic of hard rocks make it difficult to make predictions based on observations made during the usual research periods (Kennedy et al. 2017), usually of a few years. In addition to the marine action and the weathering of the cliff (Trenhaile 1987; Sunamura 1992; Masselink and Hughes 2003), the influence of the lithology and geological structure of the bedrock must be considered (see, for example, Duperret et al. 2004; Mortimore et al. 2008; De Pippo et al. 2008; Del Río and Gracia 2009; Swirad et al. 2016). In the current context of climate change, an impact in the medium and long term on the current coasts and their geomorphology because of sea level rise (e.g., Church et al. 2013; Kopp et al. 2014; Le Bars et al. 2017) and marked changes in climate (general increase in temperatures, marked change in the rainfall pattern, increased frequency of storms, changes in the wind regime, etc.; see Dufresne et al. 2013; Noël et al. 2021) is expected. There is extensive literature on the effects that these changes will have on low-lying coastal areas (e.g., Trenhaile 2002; Davidson-Arnott 2010; Nicholls and Cazenave 2010; Nicholls et al. 2021; Slangen et al. 2012; Ranasinghe 2016; Bon de Sousa et al. 2018; Sanjosé Blasco et al. 2018; Lauzon et al. 2019; Scardino et al. 2020). However, the effects on rocky coasts have received much less study, even though they make up more than half of the world's coasts (Griggs and Trenhaile 1994; Young et al. 2009; Young and Carilli 2019). The reason for this is the slow recession of these coasts in comparison to the rapid retreat of sandy shores (Moura et al. 2006; Swirad et al. 2016; Trenhaile 2016).

✉ Carlos López-Fernández
lopezcarlos@uniovi.es

[1] Department of Geology, University of Oviedo, Oviedo, Spain

[2] Department of Mining Exploitation and Prospecting, University of Oviedo, Oviedo, Spain

[3] Department of Geodynamics, University of Granada, Granada, Spain

It is known that the rates of rocky cliff retreat vary widely as a result of the many variables involved in their evolution. Prémaillon et al. (2018) proposes median erosion rates of 2.9 cm yr^{-1} for hard rocks, 10 cm yr^{-1} for medium rocks and 23 cm yr^{-1} for weak rocks. Since the 1980s, the north Atlantic coast of Spain (Fig. 1a) has been the subject of studies focused on sandy bays, estuaries, and marine terraces, especially in its central zone (e.g., Flor and Flor-Blanco 2006; Codrón and Rasilla Álvarez 2006; Flor-Blanco et al. 2015, 2016; Sanjosé Blasco et al. 2020). Recently, the results obtained in cliffs formed in Paleozoic and Jurassic rocks in this sector have shown that they evolve mainly by rotational and planar landslides, with estimated coastline retreat velocities in specific areas at Cabo Peñas (55 km East of the studied cliff) of up to 2.19 m in lutite and limolite for 2006–2017 (Domínguez-Cuesta et al. 2020a) or active mass movements of more than 70,000 m^2 extension in cliffs that have developed in Jurassic marl and sandstone located 100 km East of the cliff that is the object of this study (Mora et al. 2018; Domínguez-Cuesta et al. 2020b). However, instabilities and rates of retreat of cliff faces on the west Cantabrian coast that have formed in other rocks, such as relatively

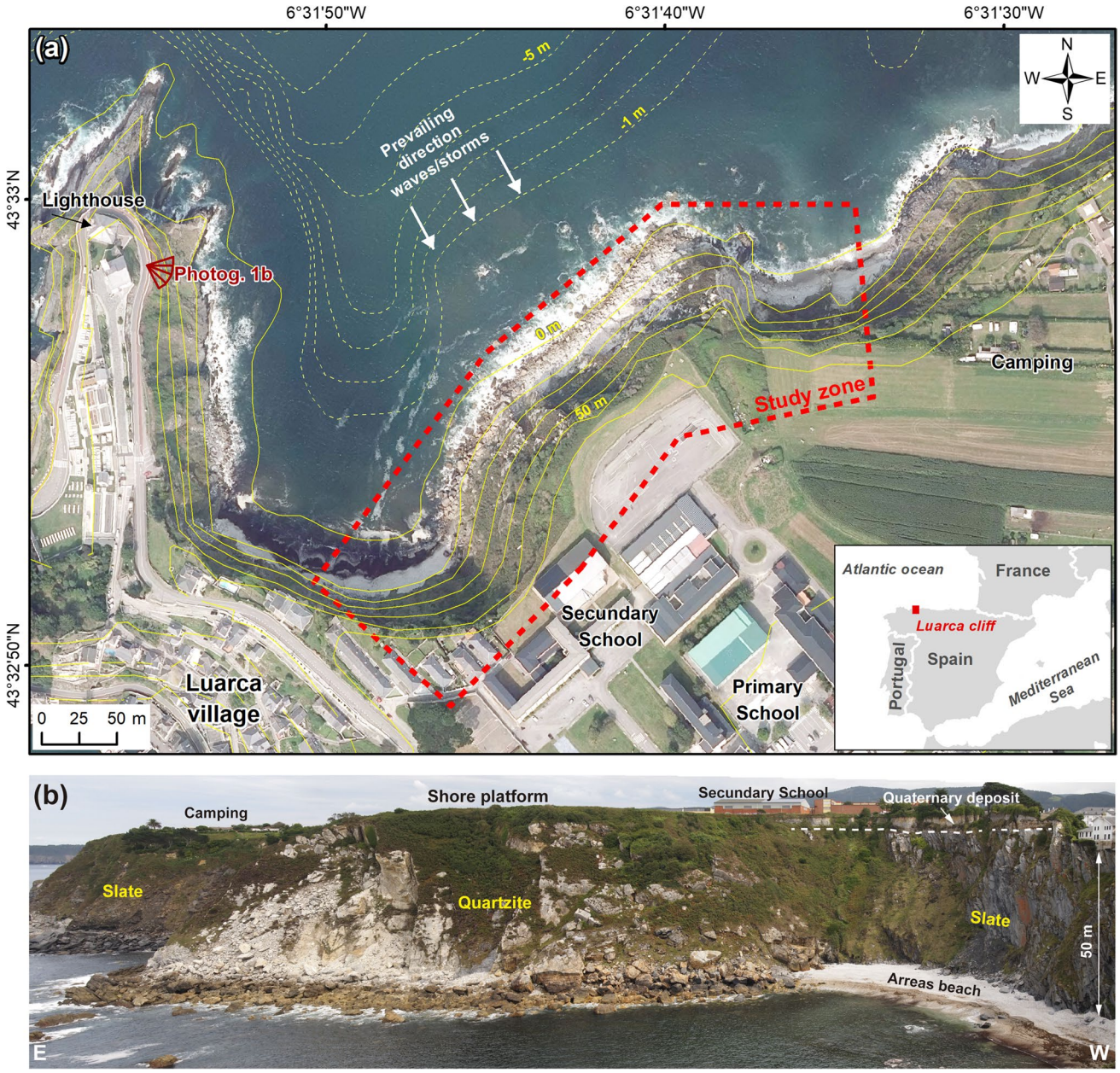

Fig. 1 **a** Location of the studied sector of the Luarca cliff (NW Atlantic Coast of Spain); (**b**) Panoramic view of the cliff from lighthouse (see location in 1(a))

hard Ordovician metamorphic rocks, remain unknown. The western and central sectors of the Cantabrian Coast are also locally affected by port activities, whose related structures are also subject to marine erosion (Flor et al. 2006), and have an important cultural heritage (e.g., Iron Age and Roman hillforts located on cliff peninsulas) that is being destroyed by marine erosion (Camino Mayor 1995; Jiménez-Sánchez and Ballesteros 2017; Domínguez-Cuesta et al. 2020a).

This research aims to contribute to the understanding of the geomorphological evolution of coastal cliffs that have developed in hard rocks. A rocky cliff located in Luarca (Fig. 1), which is representative of cliffs formed in Ordovician slate and quartzite on the Western Cantabrian Coast, has been selected as a case study. Given its complex geological features, it can serve to reveal the "attacking" or "defensive" role played by structural, lithological, and geomorphological factors in cliff retreat. This requires a necessary characterization of the instability processes, including their spatial and temporal delimitation, as well as the quantification of the contribution of these processes to the general retreat.

Setting

The cliffs of Luarca (extending for 4,500 m^2) are located on the Northwest Atlantic Coast of Spain (Fig. 1a), a sector dominated by rocky cliffs interrupted by small sandy beaches and narrow estuaries (e.g., Flor-Blanco et al. 2015). The base of the cliff is connected to the current abrasion platform, its upper edge being the northern limit of ancient marine terraces, locally known as "*rasas*". These surfaces extend, with a width of 2–6 km, along more than 200 km of the coast and have an elevation of between 100 and 150 m in their eastern part, which progressively decreases towards the West (e.g., Moñino et al. 1988; Álvarez-Marrón et al. 2008; Flor and Flor-Blanco 2014; Ballesteros et al. 2017; Domínguez-Cuesta et al. 2015; López-Fernández et al. 2020). *Rasas* and the corresponding cliffs are the result of the emersion of the old abrasion platform, which originated during the Pleistocene, with an uplift rate since then of 0.1–0.2 mm·$year^{-1}$ (Jiménez-Sánchez et al. 2006; Álvarez-Marrón et al. 2008).

The approximately 570 m long section of cliff in this study is located East of the village of Luarca (ca. 6,000 inhabitants in 2021). The section shows a general N43°E direction and reaches a height of 67 m (Fig. 1a). In general, the upper part of the cliff is notably steep, sometimes vertical, while its lower part is inclined towards the sea with a variable slope (58°NW on average). The slope is partially covered by detached fallen blocks. Those blocks located at the cliff foot, which cover the current abrasion platform (inclined 3°N), are directly affected by marine action (Fig. 1b). The upper edge of the cliff is the North limit of the rasa, which in this area has a 3 km width and dips 0.5°N. The slope is covered by small, scattered plant communities. These are shrubby and are in the middle and upper part of the cliff, as they are more protected there.

The climate of the study site is oceanic, temperate and without a dry season. Rainfall is regularly distributed throughout the year and averages 1,404 mm according to the State Meteorological Agency of Spain-*Agencia Estatal de Meteorología* (AEMET). The annual average temperature is 13.7 °C, oscillating between average minimum and maximum values of 9.6 and 18.0 °C. Prevailing winds come from the Southwest, although those responsible for modelling the coastline, given the orientation of the coast (West–East), are those of the West and Northwest component, generally very intense. The dominant waves are from the Northwest, with an average annual wave height of 1.5 m, with the median at 1.5–2 m and the P95 at 4–4.5 m. In this coastal sector, waves with heights significantly greater than 1.7 m are considered stormy, with maximum values of around 10–12 m, associated with storms with a West and Northwest component, frequent in winter (Izaguirre et al. 2011). The average annual wave period is 9 s, and 95% of the time it is less than 12 s. The coast shows semi-daily tidal variations between 1.00 and 4.65 m, although in extreme circumstances they reach 4.95 m. In general, the high tide allows the swell to impact the rocky deposits at the foot of the cliff and even the base of the cliff during storm events. On this coast the waves and tides cause a generalized transport of sediments to the East (Flor and Flor-Blanco 2005), with the consequent local topographic effects motivated by the presence of capes and inlets.

The area above the Luarca cliffs, as in other areas of the Atlantic Coast, is mostly subject to urban development. Beyond a point less than 5 m from the edge of the cliff, dozens of houses, a secondary school and a primary school, and tourist complexes have been built in the area in recent decades, progressively displacing the traditional agricultural use.

The cliff bedrock resulted from a complex geological history derived from the overlapping of two orogenies (Variscan and Alpine) and the different rheological response of the metamorphic rocks. The bedrock of the central sector of the cliff is quartzite, while slate outcrops at its eastern and western ends; both are Middle Ordovician in age and belong to the Luarca Formation (Marcos 1973; Gutiérrez-Marco et al. 1999). Quartzite layers adopt a Northeast-Southwest direction, dipping Northwest and are intensely fractured. Slate layers outcropping in the cliff are oriented North–South with a subvertical dip and present a tectonic foliation whose orientation and dip vary substantially depending on the folds and faults affecting these rocks. The slate is fine-grained, black, and locally rich in iron sulphides. This rock presents an average weight density of 26.4 kN/m^3 and its uniaxial compressive strength is between 20 and 35 MPa (according to our tests); therefore,

the slate is classified as a soft rock (according to ISRM 1981) or a very low- resistance rock (according to Bieniawski 1989). The quartzite exhibits medium to coarse grain size and intense recrystallization; its average density is 26.5 kN/m^3, showing a tensile strength of 20–28 MPa and an average uniaxial compressive strength of 135 MPa (according to our previous tests); thus, the quartzite is considered a very hard rock (ISRM 1981) or a high strength rock (Bieniawski 1989). In the sector studied, the slate areas correspond to coves and beaches, while the quartzite gives rise to a small promontory, with detached blocks accumulating at the foot of the cliff. Covering the bedrock, less than 3 m of Quaternary marine deposits appear on the rasa and are mainly made up of sand, rounded and subrounded quartzite pebbles and cobbles (Flor and Flor-Blanco 2014).

Methods

The methodology of the Luarca cliff study includes geomorphological mapping assisted by Remotely Piloted Aircraft (RPA), evaluation of the lithological and structural influence and the compilation of temporal evolution evidence.

Geomorphological mapping assisted by RPA

To identify the instability zones and processes, a detailed geomorphological map of the study cliff was created at a 1:2,000 scale in a Geographical Information System (GIS, ArcGIS Desktop v10.3), combining field evidence and data acquired by RPA. The cartography exhibits the spatial distribution of the features and deposits linked to instability processes or marine action. The upper edge of the cliff, the limit of the current abrasion platform and the scour zone at the foot of the cliff have also been delimited. The RPA provided a Digital Elevation Model (DEM) (8 cm spatial resolution) and an orthophotograph (3 cm resolution) of the study area corresponding to two photogrammetric surveys carried out in November 2018 and December 2020.

The RPA was operated by the company INGECOR Geomatics (Fig. 2a) using a CÁRABO S3 (ICOM3D), a quadcopter with a Sony A5100 with Exmor® CMOS Sensor type APS-C (23.5 × 15.6 mm), and a 20 mm fixed lens. From a flight height of 111 m, 147 images were taken (ground resolution of 2 cm / pix), establishing 9 control points (fixed targets). As observational instruments, two GNSS Topcon GR3 receivers (Antenna TPSGR3 NONE) were used, and the data collected from a permanent station located at 100 m (Antenna LEIAX1203 + GNSS NONE) were also incorporated. Image processing was carried out with Agisoft Metashape v.1.5.2 software. The maximum error calculated from the control points was 3.52 cm. For each flight, a textured 3D cloud (126,462 points) with an average point density of 157 points/m^2 was generated. The Cloud Compare v.2.10.2 open-source program (available at http://www.cloudcompare.org) was used to analyse the point cloud obtained with the RPA. This software made it possible to identify and measure the bedrock discontinuities. The application of this technique allowed the acquisition of structural measurements in areas inaccessible to traditional field methods. It also makes it possible to carry out comprehensive digital analyses and optimize the time spent on data collection.

Geological mapping and structural analysis

To establish the contribution of the lithological and structural factors to the stability of the cliff, a geological map was made at a scale of 1:2,000, based on field work and the information provided by the RPA. Geological structure was complemented by four geomechanical stations; two stations on the slate and two on the quartzite bedrock. In each station, discontinuity families (stratification, joints, faults, foliations) were identified, detailing their dip, dip direction, spacing, opening, roughness and infill. Furthermore, structural data were collected at 57 inaccessible points on the cliff surface from the point cloud obtained with the RPA through the Compass plugin (Thiele et al., 2017) of the Cloud Compare software. This powerful program allowed the identification, positioning and measurement (dip/dip direction) of flat surfaces of geological origin (Fig. 2b). The DIPS v.8.020 (Rocscience) program was used for the geometric and kinematic analysis of the discontinuities. With this software, the discontinuities were analysed using stereographic projection (equal area, lower hemisphere), allowing us to determine the potential formation of wedges, rockslides, and other instabilities. Stereographic projection is a type of azimuth conformal projection that allows the representation of three-dimensional objects (e.g., joints, bedding) on a two-dimensional surface and the performance of linear, angular, and surface measurements.

Cliff monitoring

The Luarca cliffs were monitored to survey block displacements and coastline retreat. The information used for this was collected through historical orthophotos (taken in 2003, 2006, 2009, 2011 and 2014; National Plan for Aerial Orthophotography of Spain, available at http://centrodedescargas.cnig.es/CentroDescargas), orthophotos acquired via RPA (2018–2020) and field campaigns using a total station (2018–2022). All images have a spatial resolution of 0.25 m, except for the 2003 and 2018/2020 flights, whose resolution is 0.5 m and 0.08 m, respectively. All the orthophotographs were integrated into GIS to undertake a comparative study for the period 2003–2020, taking the upper edge of the cliff and the spatial location of detached and identifiable blocks as a reference.

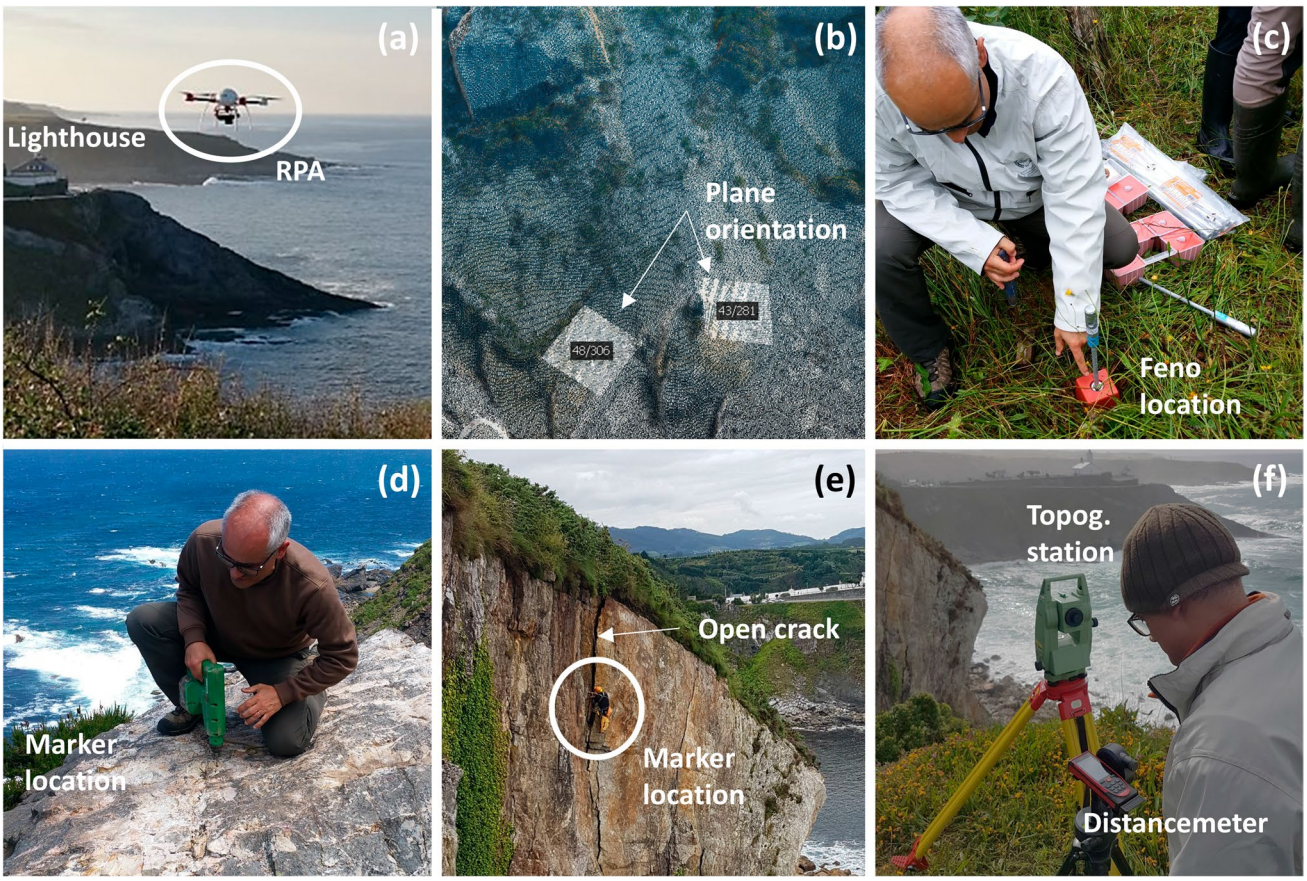

Fig. 2 **a** Photogrammetric flight in November 2018; (**b**) Determination of the dip/dip direction of a plane in the Cloud Compare program; (**c**) Installation of feno topographic markers on the upper edge of the cliff, (**d**) control points in detached blocks and (**e**) in a vertical crack; (**f**) Total station and laser distance meter used in the cliff monitoring

A high-precision quantitative comparative study was carried out between the DEM obtained by RPAs (Fig. 2a) in November 2018 and August 2020. This allowed us to identify the geomorphological changes that the cliff underwent in that period using the M3C2 plugin of the Cloud Compare program. This tool calculates the local distance between two-point clouds along the surface normal direction that tracks 3D variations in surface orientation (Lague et al. 2013).

Moreover, topographical monitoring of the slope was carried out, consisting of the installation and surveying of 20 control points distributed along the cliff (Table 1). Seven feno markers were installed on the upper edge of the cliff (Fig. 2c). Each marker consists of a 50 cm long galvanized bar with a resin head and triple extensible anchor, driven into the ground by striking. Another eight topographic nails were drilled in rocky detached blocks in the eastern cliff (Fig. 2d), together with the opening of a vertical crack in the upper escarpment of the same sector, where five control nails were installed (Fig. 2e). The measurements were taken from June 2018 to April 2022, and eleven measurements were made at approximately five-month intervals (Table S-1, supplementary material). A Leica TC-407 total station was used (angular measurement precision = 7 "; distance measurement precision: + 2 mm + 2 ppm) (Fig. 2f). Displacements less than 3 cm are not considered significant considering the terrain configuration and the methodology used.

Results

The results are summarized below, including spatial distribution and geomorphological evidence of cliff slope instability, characterization of the lithology and structure of the area and the temporal evolution of the cliff.

Cliff slope instability: spatial distribution and geomorphological evidence

Geomorphological mapping (Fig. 3a, b) shows the existence of mass movements in 72% of the cliff. Translational landslides are the most widespread process, followed by rockslides and topples, which are mainly concentrated in its eastern part and, in part, in the central sector. In the eastern sector, small flows

Table 1 Topographic markers installed on the cliff. Coordinate system: ETRS-89 29 N; mean reference altitude: Mediterranean Sea in Alicante (Spain). Measurement dates: 2018–11-jul, 2018–29-oct, 2019–18-jan, 2019–26-apr, 2019–12-jul, 2019–05-dec, 2020–18-jun, 2020–18-dec, 2021–24-may, 2021–16-jul, and 2022–29-apr

Type	Situation	Control point	Installation date	UTM coordinates (m)		
				X	Y	Z
Base	Upper edge of the cliff	B1	2018–11-jul	699,746.44	4,824,736.37	69.68
Feno marker		F1	2018–11-jul	699,609.64	4,824,580.34	68.92
		F2	2018–11-jul	699,639.66	4,824,631.15	69.62
		F3	2018–11-jul	699,646.24	4,824,672.63	70.13
		F4	2018–11-jul	699,681.07	4,824,698.79	70.24
		F5	2018–19-jun	699,704.91	4,824,730.34	68.62
		F6	2018–11-jul	699,700.34	4,824,736.45	64.68
		F7	2018–11-jul	699,698.66	4,824,741.38	63.70
Marker	Detached blocks	C1	2018–19-jun	699,737.58	4,824,756.32	63.35
		C2	2018–19-jun	699,727.72	4,824,755.28	60.68
		C3	2018–19-jun	699,726.01	4,824,759.23	59.85
		C4	2018–19-jun	699,730.78	4,824,762.46	58.89
		C5	2018–19-jun	699,727.07	4,824,764.89	55.99
		C6	2018–19-jun	699,729.12	4,824,767.29	57.58
		C7	2018–19-jun	699,725.09	4,824,771.94	52.53
Marker	Open tension crack	A1	2018–11-jul	699,699.04	4,824,743.67	61.66
		A2	2018–11-jul	699,700.14	4,824,743.21	61.88
		A3	2018–11-jul	699,699.33	4,824,743.34	59.03
		A4	2018–11-jul	699,700.06	4,824,742.87	59.39
		A5	2018–11-jul	699,699.27	4,824,743.07	56.91

of debris, debris slides, and rock falls associated with two high angle faults affecting the bedrock are also observed. At the cliff foot, parallel to its base and approximately 300 m in length and 40 m wide, there is a main strip of accumulation of rocky blocks mobilized from different parts of the cliff, which are currently being affected by marine action (Fig. 3a, b). A scour zone, whose morphology responds to an origin linked to wave action, is observed on these deposits, located 20–25 m from the base of the rocky cliff. In the western and eastern sectors of the cliff there are two beach deposits, made up of sand and pebbles; the former is 150 m long and 45 m wide, while the latter covers an area 100 m long and 40 m wide.

Cliff structure and lithology

The geological map shows the general N27°E orientation of the more than 300 m thick quartzite succession that forms the main part of the study cliff (Fig. 3c). The layers range from a few decimetres to 4 m thick and dip between 35° and 60° to the Northwest. The base and top of the quartzite succession exhibit two successions of slate, with a similar orientation to the quartzite and with a dip of between 40° and 80° towards the West-Northwest. The contact between the two lithologies is net. The slate is hundreds of meters thick and occurs in massive form, it being possible to identify the stratification planes (S0) only within sandy layers. In addition, the slate shows a marked tectonic foliation (S1) caused by the orientation of the phyllosilicates and quartz during the Variscan Orogeny.

Five families of discontinuities have been recognized in the quartzite: the bedding (S0) and four families of joints (J1 to J4), whose main characteristics are detailed in Table 2 and Fig. 4. The J1 family is the most abundant, followed by J2 and the other families. In general, the J1 J2 and J3 families include mainly subvertical fractures-oriented NE-E-SE, while the J4 family comprises fractures with NE strike and a mean dip of 42°. Near the eastern contact with the slate, two faults (parallel to the bedding and inclined 65°NW) are observed in the quartzite. In this sector the bedrock shows (in a band of approximately 50 m width) intense fracturing, associated with these structures.

In the slate, the foliation (S1) is the predominant discontinuity, whose disposition is controlled by the folds that affect these rocks; thus, a range of orientations from E-W to NE-SW with dips between 29 and 42° can be observed. Locally, some bedding planes and a family of subvertical discontinuities with NE strike are identified.

Evidence of temporal evolution

Cliff evolution in 2003–2020 based on orthophotographs

The analysis of the sequence of seven orthophotographs corresponding to the period 2003–2020 confirmed the overall stability of the upper edge of the cliff, both in slate and quartzite. Only a single change can be observed in the upper part of the vertical escarpment located in the easternmost part of the cliff, in the contact zone between

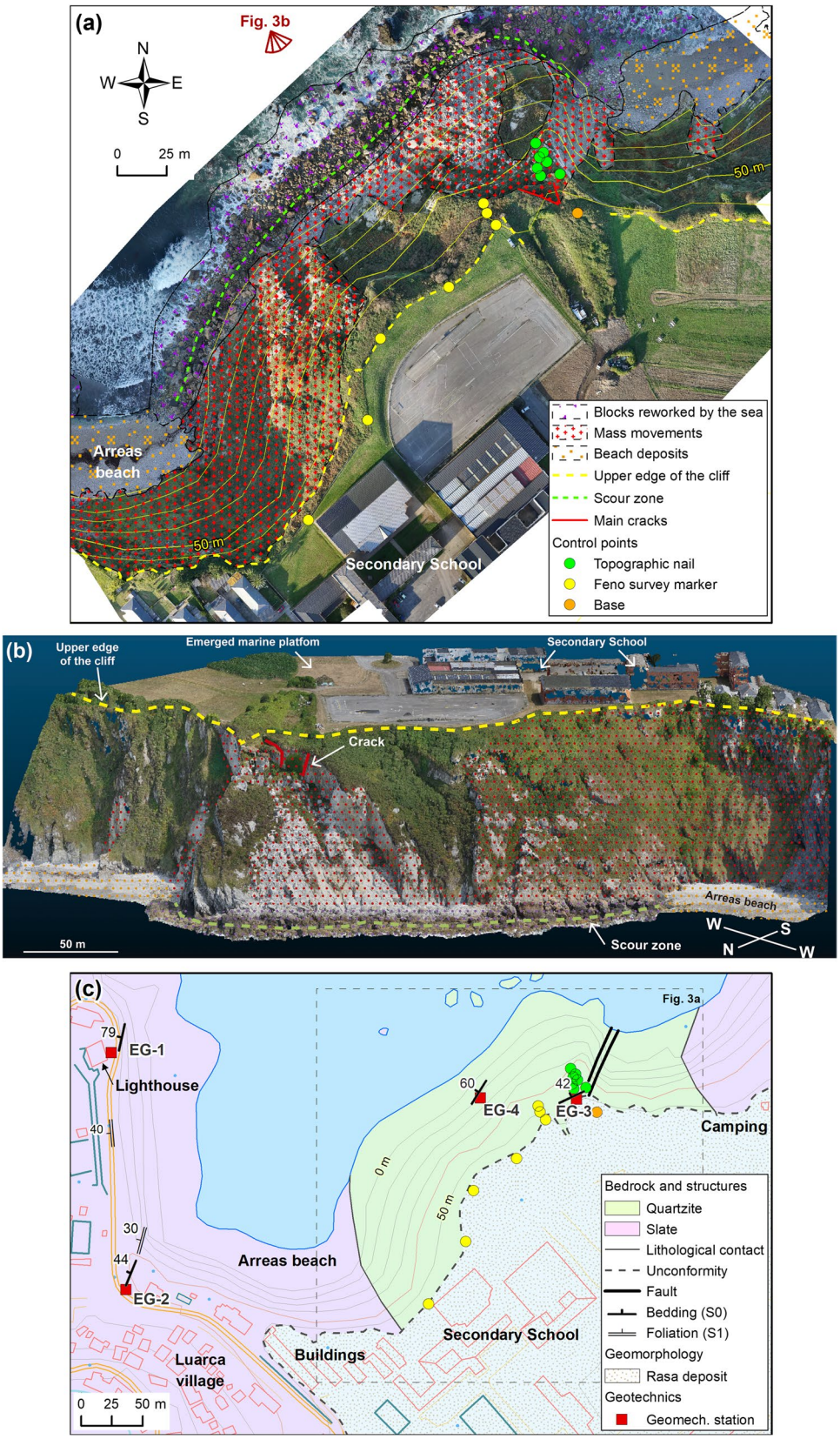

Fig. 3 **a** Geomorphological map and (**b**) cliff view showing areas affected by mass movements. **c** Geological map showing monitoring points and geomechanical stations

Table 2 Main characteristics of the families of discontinuities affecting the study cliff bedrock. All parameters are defined according to Bieniawski (1989)

Lithology	Discontinuity family	Mean Dip/Dip direction (°)	Mean spacing	Mean opening	Mean roughness
Quartzite	S0 (bedding)	52/297	0.75 m	> 0.5 mm	V-type, smooth wavy
	J1 (joint)	84/022			
	J2 (joint)	81/118			
	J3 (joint)	74/159			
	J4 (joint)	42/116			
Slate	S0 (bedding)	86/103	-	Closed	IX-type, slickensided
	S1 (foliation)	29–42/103–296	-	Closed	
	J1 (joint)	88/14	0.5 m	< 1 mm	

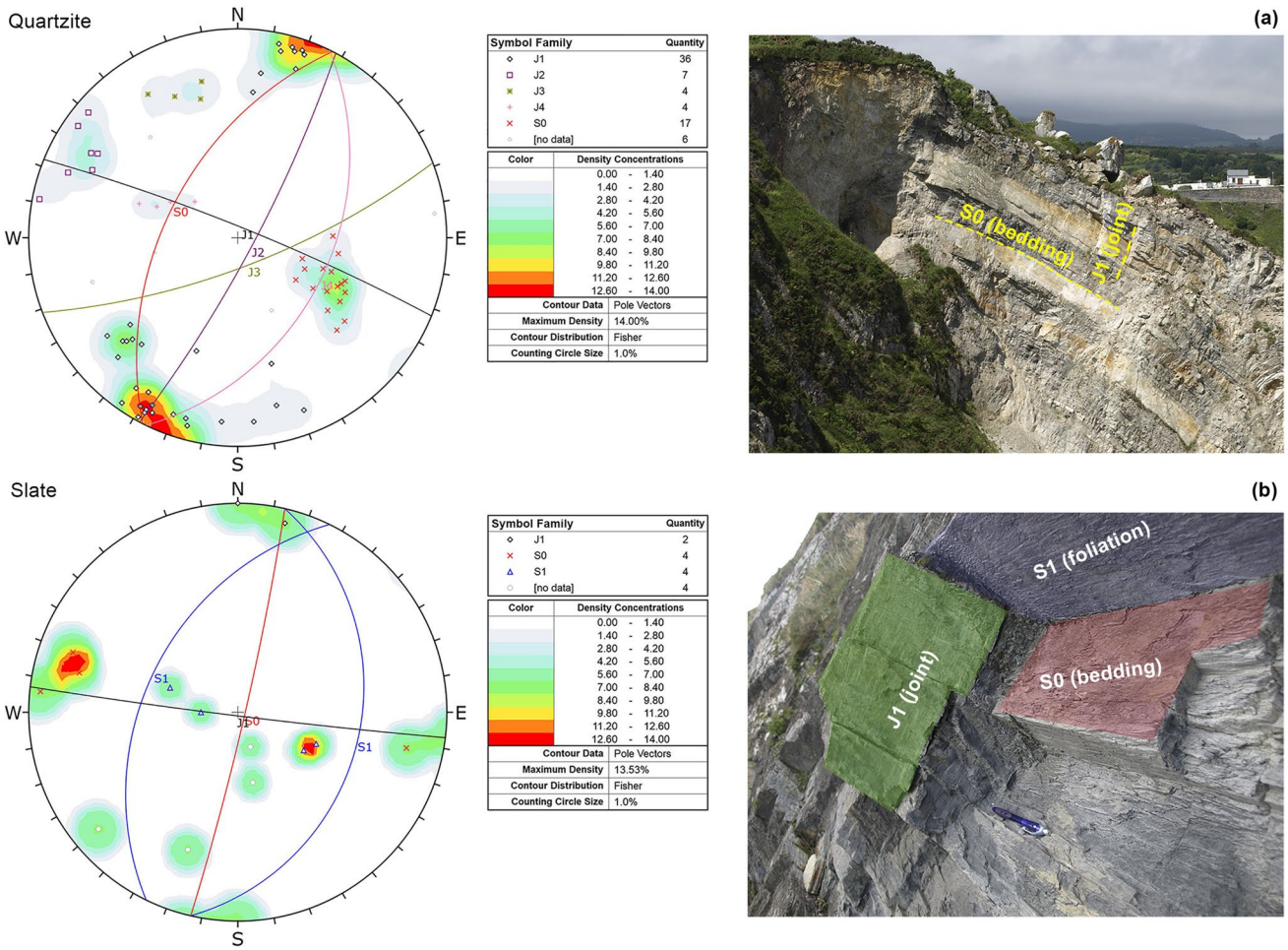

Fig. 4 Stereographic projection of the structural data of the (**a**) quartzite and (**b**) slate acquired by means of four geomechanical stations (31 measurements) and points cloud (57 measurements). The lines correspond to the midplane of each family of discontinuities. The poles of each plane and their probability distribution according to von Mises-Fisher (Tanabe et al., 2007) are also shown. The right side shows the field appearance of the quartzite bedrock at the NE end of the cliff and of the slate at EG-1

quartzite and slate (Fig. 5). Between 2003 and 2011, the detachment of a sector 17 m long and 5 m wide, mobilizing an area of 85 m^2 in extension, was observed (red arrows in Fig. 5b). The detached material, mainly centimetre and decimetre-sized blocks, was quickly reworked by marine action. Based on this observation, a maximum retreat rate of 0.47 $m{\cdot}year^{-1}$ could be estimated in this small sector for the period 2003–2020. In this zone, the lower part of the cliff was affected by three mass movements: (i) a landslide (300 m^2) located in the eastern cliff and first observed in 2011, showing displacements of up to 6 m in 2014 and up to 4 m between 2014 and 2018; (ii) a second movement (198 m^2) is located in the westernmost area and had already been observed in the first orthophoto analysed (2003), showing displacements of 7 m over three years (130 m^2), and of 6 m in the following five years (68 m^2); and (iii) a new movement (140 m^2) was observed to the East in 2018. As in the previous case, the detached material (centimetre and decimetre size) was quickly reworked by the marine action that mainly affects the base of the cliff during storms.

In the central cliff, the movement of a rock block that slid 16 m westward following a stratification plane, from 23 to 7 m elevation between 2011 and 2014, is observed (black arrow in Fig. 5c). This block, very resistant to marine action given its size, is now part of the deposit of metric-sized blocks accumulated at the foot of the cliff. Likewise, between 2018 and 2020, centimetre-size blocks were detached from an escarpment located further to the Northwest (Figs. 5 and 6). The detached material remains deposited on the lower part of the cliff and is only affected by major marine storms. At the bottom of the western part of the cliff, translational sliding, and rotation of two blocks (3 and 7 m diameter) was observed between 2014–2020 (yellow arrows in Fig. 5d). Additionally, decimetric rockfalls were observed in the western cliff from the slate escarpments between 2003 and 2020. These blocks are now deposited on top of beach sediments, forming the western boundary of the block deposit at the foot of the quartzite cliff. Finally, during this period, no significant movement of the quartzite blocks located at the cliff bottom was observed, not even of the blocks most directly exposed to marine action.

Cliff evolution in 2018–2020 based on a quantitative comparison between high precision DEM

The comparison made using the M3C2-CloudCompare plugin between high-precision DEMs (8 cm pixel) acquired using RPA in November 2018 and in November 2020 has made it possible to quantify the evolution of the cliff over two years. For this analysis, considering the characteristics of the point cloud and the cliff, as well as the expected movements, a normal diameter of 1 m, a projection diameter of 1 m, and a projection depth of 6 m were used. Almost the entire cliff shows stability during this period, except for small occasional changes. These changes occur in the central and lower part of the cliff (dashed red box in Fig. 7), corresponding to debris deposits detached from a vertical escarpment in 2018–2020 (see Fig. 6), as shown by the sequential analysis of orthophotographs (see Fig. 5). Variations associated with translational sliding of blocks dislodged by marine action between 2014 and 2020 are also observed at the base of the western cliff (dashed white box in Fig. 7; Fig. 5d). Finally, in the western part, slate rock falls are observed (dashed orange box in Fig. 7). In the rest of the studied area, the differences observed between the two DEM correspond mainly to changes in vegetation, isolated blocks and beach deposits.

Cliff evolution in 2018–2021 based on topographic monitoring

The detailed analysis of the seven monitoring campaigns confirms that the measured movements of the control points between July 2018 and April 2022 (Table 3. Complete data in Table S-1, supplementary material; see location in Fig. 3) are within the error range of the technique used, no displacements in the same orientation > 3 cm being observed. Greater movements are only visible at points F1 and F6, which are explained by damage to the control point and by a compression in the level of the topsoil since its installation, respectively. There was also no increase in the opening of the monitored vertical crack (Fig. 2e) located in the upper escarpment-oriented E-W, in the studied period.

Discussion

The influence of the conditioning factors (lithology and structure) on the variability of slope instabilities developed in the Luarca cliffs is discussed here. The spatial and temporal distribution of slope instabilities is also analysed in terms of their contribution to the cliff evolution.

Slope instability and local factors

Lithological factor

It is well known that lithology is a major conditioning factor in cliff evolution (e.g., Duperret et al. 2004; Lim et al. 2010). The resistance conferred by the properties of each type of lithology limits erosion caused mainly by wave action (Summerfield 1991; Sunamura 1992; Bird 2000; Duperret et al. 2005; Trenhaile and Kanyaya 2007; Wolters and Möller 2004) and abrasion generated by the friction of

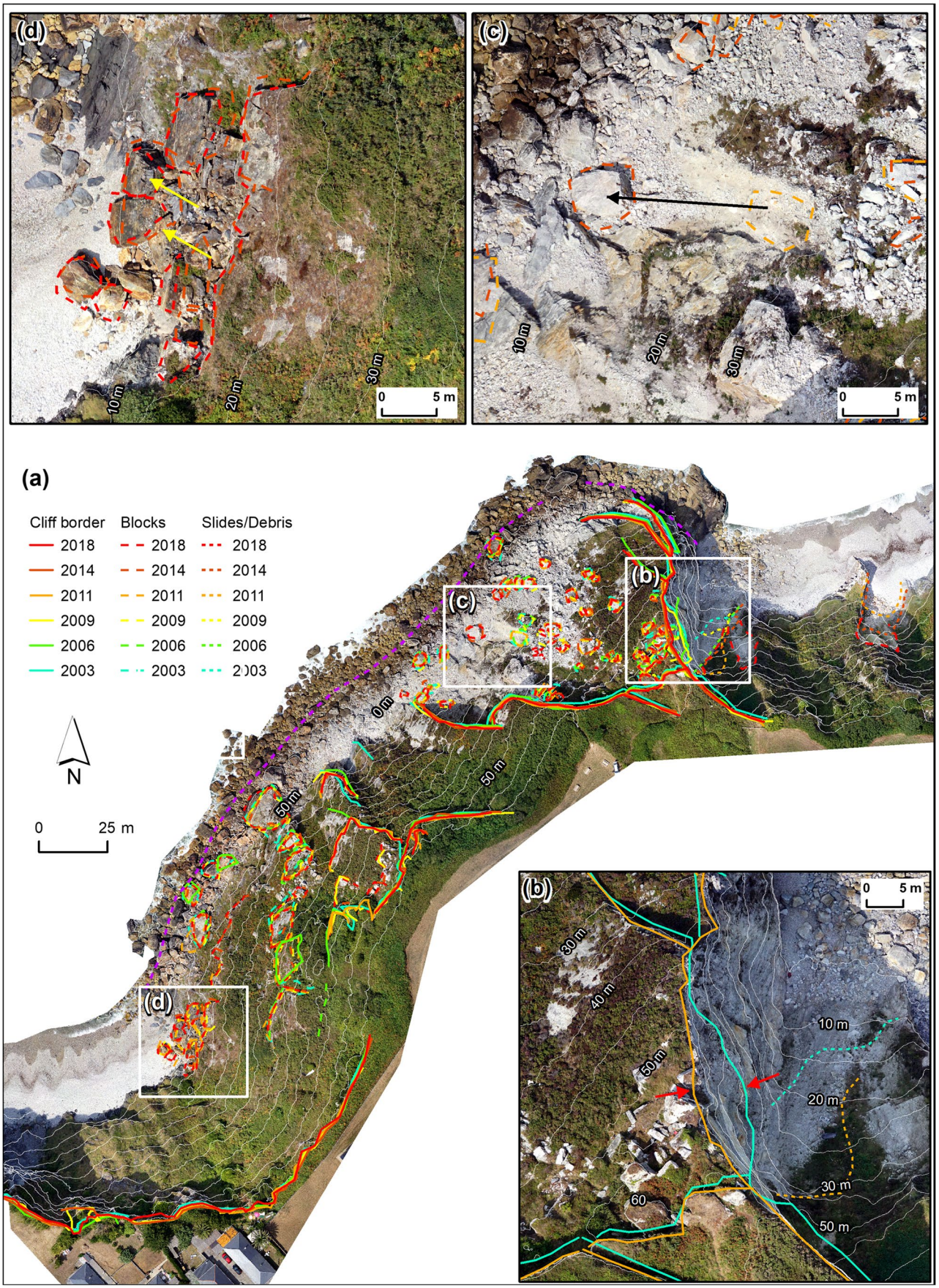
(d)
10 m
20 m
30 m
0 5 m
(c)
10 m
20 m
30 m
0 5 m
(a)
Cliff border
Blocks
Slides/Debris
2018
2014
2011
2009
2006
2003
N
0 25 m
(c)
(b)
(d)
0 m
50 m
50 m
(b)
0 5 m
30 m
40 m
50 m
10 m
20 m
30 m
60
50 m

◂**Fig. 5** **a** Evolution of the Luarca cliff over the years 2003, 2006, 2009, 2011, 2014, 2018 and 2020 shown on the 2020 orthophotograph. The scour zone is shown as a dashed purple line; (**b**) Cliff top retreat between 2003 and 2011; (**c**) y (**d**) Translational slip trajectories of quartzite blocks between 2014 and 2020

rock fragments (Trenhaile 1987 2002; Griggs and Trenhaile 1994; Komar 1998). The evolution of the Luarca cliffs is conspicuously controlled by the lithology, which acts in combination with the geological structure. The quartzite shows a relatively high resistance to erosion and the cliff that has been formed in it is mostly adapted to the bedrock structure. The quartzite blocks detached and accumulated at the cliff foot act as a natural defence against marine action (owing to their high abrasion resistance and high angle of internal friction). Direct wave action acts mainly on this block deposit even at high tide, only reaching the cliff base during the strongest sea storms. An incipient scour zone has been detected in these blocks located at the foot of the cliff through geomorphological mapping (Figs. 3a, 5a and 6b). Thus, these deposits are slowing down the cliff retreat, even in the part most exposed to sea storms from the NW. Slate is substantially less resistant to marine erosion than quartzite, which leads to the development of vertical faces and even overhangs. The detached slate blocks and cobbles are easily reworked and eroded by marine action, allowing the waves to impact directly on the cliff bottom; here sandy beach deposits appear.

The role of discontinuities

The distribution of the discontinuities (bedding, faults, joints, and foliation) that affect the bedrock, together with the orientation of the coast, condition the instability mechanisms that affect the Luarca cliffs in a different way. The slate (with a more ductile behaviour against tectonic deformation) shows only three families of discontinuities (S0, S1 and J1), whereas five families of discontinuities were recognised in the quartzite (S0, J1 to J4). In most of the cliff, the position of the quartzite stratification (inclined 30–35° towards the sea) controls the occurrence of translational block slides, the main instability process affecting the cliff (Fig. 8a). Along the cliff there are numerous detached blocks showing slope instability movements that we interpret as episodic according to their distribution by slope (Figs. 5a, c, 8b and 9a, b). The detached blocks remain for an indeterminate time (depending on several variables) on the cliff slope until they reach the base of the cliff and become part of the deposit at the foot of the cliff. This deposit is already affected by marine action (Figs. 5d and 9a, b). The individualization and detachment of the prismatic rocky blocks is a consequence of the intersection of the discontinuity families (mainly S0, J1, J2), while their size (with an average thickness of approximately 1 m and dimensions that reach 7 × 5 m) is determined by the spacing of each joint family. In the upper part of the cliff, tension cracks with centimetric openings are frequent, delimiting rocky blocks that are in an incipient phase of sliding. Marine action, which in this area mainly involves the action of marine waves coming from the NW and orthogonal to the cliff, acts on the discontinuities, favouring their opening (due to the impact of the waves on the air/water inside) and the progression of weathering. Gradually, the cliff bottom is undermined, and the quartzite layers are undercut, which allows and favours the blocks' sliding. This process, which progresses towards the cliff top and causes its retreat, is slowed down as a result of the natural defence against marine action provided by the accumulation of quartzite blocks at the cliff foot.

In areas where the cliff has a subvertical slope, the intersection between discontinuities leads to the formation of wedges and their subsequent topple/detachment by free fall and, sometimes, planar sliding towards the base of the escarpments (Figs. 5a, b, and 8b). In some sectors (such as the easternmost area), there is a high density of bedrock fracturing, resulting in the formation of centimetre to decimetre-sized blocks that accumulate at the foot of the cliff as result of debris slide and debris flow of small dimensions (< 10–15 m wide). The brecciation observed in the bedrock seems to be related to the existence of two faults (parallel to the strike of the stratification but with a steeper dip, 65° NW); these structures with an original reverse fault movement (according to the drag folds that can be seen in the quartzite layers), act as sliding surfaces favouring the instability that affects the central cliff sector (Figs. 8b and 9b).

In summary, the disposition, continuity and opening of the discontinuities of the bedrock of the Luarca cliffs are factors that control their erosion, which would be much less efficient in a massive or slightly fractured bedrock. The results obtained in the Luarca cliffs are analogous, for example, to studies on coastal cliffs on the Italian island of Favignana (Iannucci et al. 2017), on the Norwegian coast (Braathen et al. 2004), on the Scottish coast (Ballantyne et al. 2018), or in Portugal (Epifânio et al. 2014).

Moreover, Donelan et al. (1996), Davidson-Arnott (2010), Limber and Murray (2011), Terefenko and Terefenko (2014) and Gerivani and Savari (2019) reported similar results on the role played by the orientation of the cliff and the massif against the erosive efficiency of marine action. De Lange and Moon (2005) concluded that a higher number of discontinuities causes a higher rate of cliff retreat. However, the discontinuities of the Luarca cliffs play a double role: (i) facilitating the erosion of the cliff and (ii) supplying blocks that form a deposit at the foot of the cliff and which, given their high resistance and metric size, form a natural breakwater protecting the cliff from the marine erosive action of the onslaught of waves.

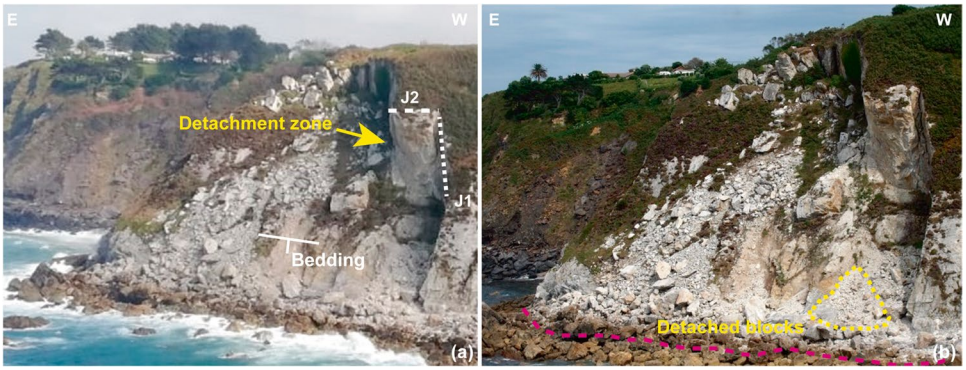

Fig. 6 Comparison between pictures of the central area of the cliff carried out in (**a**) December 2019—(**b**) August 2020. Rockfall scar evidence in the upper escarpment (yellow arrow) and the accumulated detached blocks (yellow dashed line) at the bottom of the cliff can be recognized. The scour zone is shown as a purple dashed line

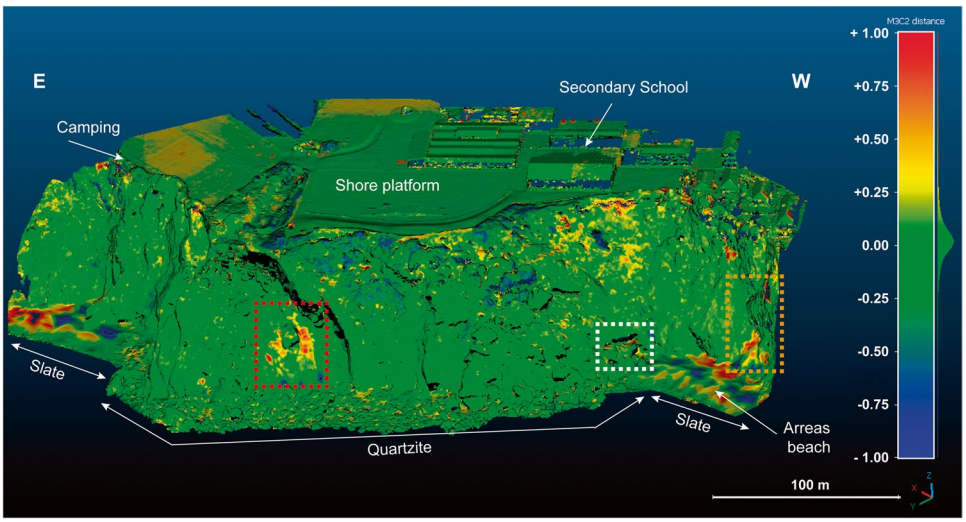

Fig. 7 Changes in the cliff between DEMs obtained in November 2018 and August 2020 established using M3C2 tool (Cloud Compare software). See text for explanations of areas remarked by squares

Spatial and temporal distribution of instabilities: contribution to cliff evolution

The Luarca cliffs have not shown a significant retreat between 2003 and 2022, as can be deduced from the analysis of the orthophotographs and topographic studies carried out, although they are affected by local instability processes. As shown by geomorphological evidence, 60% of the cliff surface presents translational landslides, which constitute the main erosion mechanism. This process affects the central-western half of the studied sector, where the direction of the layers (NE-SW) is subparallel to the coastline (perpendicular here to the main component of the prevailing storms, NW); these layers dip 30–35° towards the sea. Rockfalls are the main erosive processes within vertical slope sectors and, consequently, they are concentrated in the eastern and westernmost parts of the studied cliff (affecting 12% of the cliff), although they are also observed in the middle and upper part of the central section. At the eastern cliff foot small debris flows/debris slides affected the detached materials, which occupy an area of approximately 500 m^2.

The negligible and localized data of retreat obtained in the studied period agree with the values obtained for rocks with similar resistance to quartzite (> 20 MPa) by Sunamura (1983, 1992) or Tsujimoto (1987), who determined rates of recession ranging from 0.001 to 0.01 m·$year^{-1}$. In three sectors of the west coast of the Iberian Peninsula, similar low values were obtained on rocky coasts, including: 0.2 m·$year^{-1}$ for two years (Anfuso et al. 2007), and 0.017 m·$year^{-1}$ (1999 -2003) and 0.014 m·$year^{-1}$ (1947–2000) (Marqués 2006). However, in other points on the Cantabrian Coast (Cabo Peñas, 55 km East of Luarca), Domínguez-Cuesta et al. (2020a) obtained retreat rates of 0.57 m·$year^{-1}$ in a sandstone cliff for the period 2006–2017. Furthermore, Pérez-Alberti et al. (2013) measured retreats of 1.18 m·$year^{-1}$ in weathered granite in the extreme northwest of the Iberian Peninsula for the period 1956–2008, while Del Río and Gracia (2009) estimated rates of recession of 1.6 m·year-1 between 1956 and 2005 in southwestern Portugal. Higher values of 3.5 and 3.4 m·year-1 have been obtained by Neves (2008) and Nunes et al. (2011) on the West coast of Portugal, over several decades. These data confirm the important role played by local factors in the retreat of rocky shores.

As might be expected in a rocky cliff, all these mass movements are discontinuous in space and intermittent

Table 3 Absolute movements observed at topographic control points between the first and last measurement (July 2018—April 2022)

Location	Control point	Absolute displacement between the first and last measurement (m)			
		ΔX	ΔY	ΔZ	Δ3D
Upper edge of the cliff	F1	-0.01	0.11	-0.02	0.11
	F2	0.02	0.03	0.00	0.04
	F3	0.02	0.03	0.00	0.03
	F4	0.02	0.01	-0.01	0.02
	F5	0.02	0.00	0.00	0.02
	F6	-0.04	-0.05	-0.01	0.06
	F7	-0.03	-0.01	-0.02	0.03
Detached blocks	C1	-0.01	-0.01	0.01	0.02
	C2	-0.02	-0.01	0.01	0.03
	C3	-0.02	-0.01	0.01	0.03
	C4	-0.02	-0.01	0.01	0.02
	C5	-0.01	-0.01	0.01	0.02
	C6	-0.02	-0.01	0.01	0.02
	C7	-0.02	-0.01	0.02	0.03
Open tension crack	A1	-0.01	0.03	0.00	0.03
	A2	0.00	0.01	0.00	0.01
	A3	0.00	0.02	0.00	0.02
	A4	-0.01	0.02	0.00	0.03
	A5	-0.01	0.03	0.00	0.04

in time, as observed in other rocky coasts by Sunamura (1992), Bird (2000), or Young et al. (2009). This episodic and sudden character means that these movements escape the resolution of the land surveying techniques used in this investigation in the period of 4 years. However, this does not invalidate the application of these techniques, used successfully by other authors (Wangensteen et al. 2007; Lateh et al. 2011; Katz et al. 2011; Salvini et al. 2013; Janeras et al. 2015, Swirad and Young 2021, among others) to characterize millimetric and centimetric movements on rocky slopes, although it is necessary to address broader study periods. Thus, the comparative analysis techniques of orthophotos and DEM acquired by means of RPA corresponding to different moments in time have been revealed as more efficient in this case.

Contribution to cliff retreat research

The results obtained in this research contribute to the understanding of the instability mechanisms involved in the retreat of cliffs in hard rocks. They also contribute to understanding how local factors (mainly lithological, structural and geomorphological features) condition an episodic and sudden occurrence of instability processes (as opposed to periods of long-term stability) that affect rocky cliffs as opposed to more continuous processes, expected in homogeneous and more easily erodible lithological beds. The structural configuration and lithological nature of the bedrock play a dual role, (i) favouring the geomorphological activity that causes the cliff to retreat and (ii) slowing down marine action by providing resistant blocks of rock that form a deposit at the foot of the cliff that acts as a conservative barrier. This defensive role, conditioned by the amount of detached material, the size of the blocks and their angularity, has been studied by Trenhaile (1989, 2016) and Moses and Robinson (2011), among others. The residence time of the detached blocks on the slope and the time of reworking and erosion of the block-deposits that protect the cliff are some of the questions to be answered by future research.

Conclusions

This work has shown that the 570 m-long quartzite and slate cliffs studied in Luarca show high geomorphological activity and abundant recent evidence of instability throughout their extension. Local lithological and structural factors play an important role in the cliff evolution, which, despite being affected by intense geomorphological activity, does not show a generalized retreat in the period 2003–2022. The presence, orientation, and characteristics of the different families of discontinuities

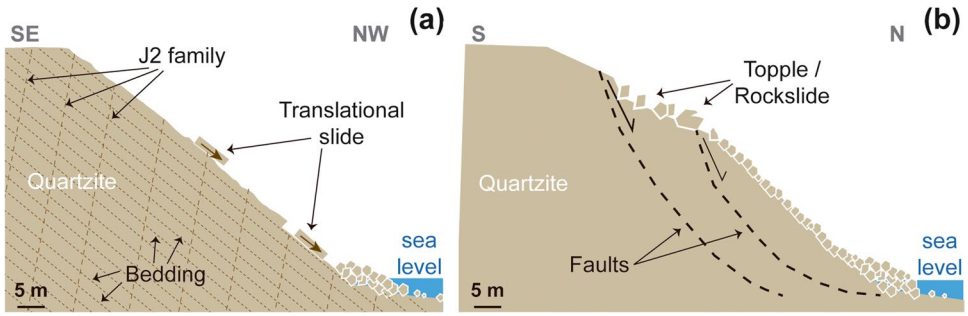

Fig. 8 Conceptual scheme of the dynamics of Luarca Cliff: (**a**) translational slides and (**b**) landslide movement in favour of two faults (parallel to the strike of the stratification but with a steeper dip) that involves the central zone of the cliff. The J1 family has an arrangement roughly parallel to the scheme

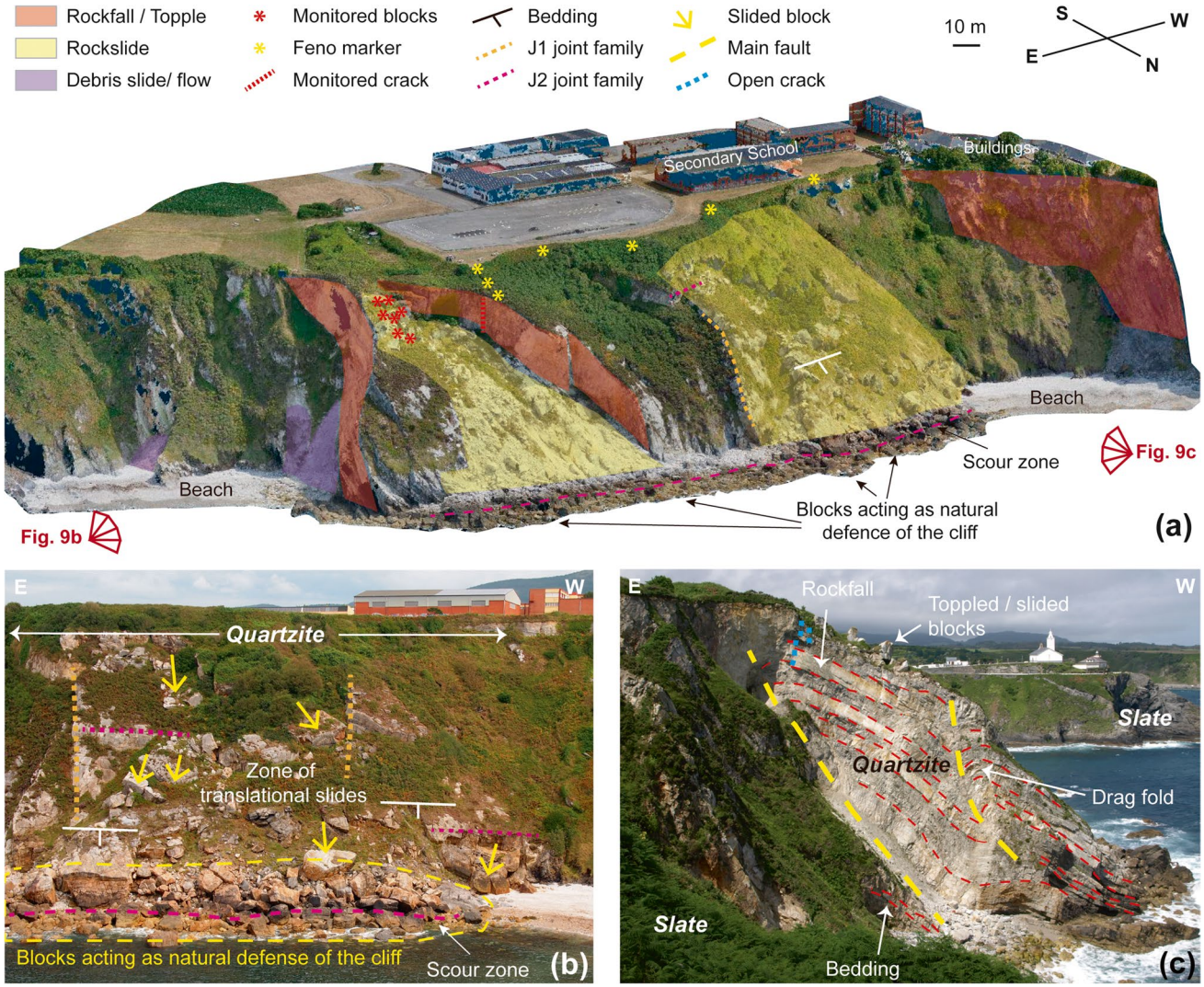

Fig. 9 **a** Main instability processes identified in the cliff. Photographic base: orthophoto acquired with the RPA in 2018; (**b**) Translational landslides in the southwestern zone of the cliff; (**c**) Structural interpretation of the vertical escarpment located in the eastern sector of the cliff

definitively condition the instability mechanisms that develop in the cliff, as well as the size of the generated blocks. Slate, affected by a smaller network of joints than quartzite, gives rise to more vertical cliffs and, given their weak nature, the detached blocks are quickly reworked and eroded by the sea, so there are no accumulations of blocks at the bottom. With respect the quartzite, structural factors condition the appearance of individualized blocks in favour of planes of weakness that are mobilized through different instability mechanisms. The blocks that reach the foot of the cliff form a deposit that acts as a natural defensive element against the erosive action of the waves and, consequently, slows down the retreat of the cliff. The time of permanence of the detached blocks on the cliff slope and the reworking and erosion of the quartzite deposits greatly exceeds the period addressed in this research, this being one of the unknowns to be cleared up in future studies.

Supplementary Information The online version contains supplementary material available at https://doi.org/10.1007/s11852-022-00907-x.

Funding Open Access funding provided thanks to the CRUE-CSIC agreement with Springer Nature. The research leading to these results received funding from (1) the "COSINES" Project [CGL2017-83909-R], Call 2017 for RETOS Projects funded by the Spanish Economy, Industry and Competitiveness Ministry-Ministerio de Economía, Industria y Competitividad (MINECO), the Spanish Research Agency-Agencia Estatal de Investigación (AEI) and the European Regional Development Found (FEDER), (2) the GEOCANCOSTA research group, supported by the Asturian Regional Government (Spain) [grant number GRUPIN-IDI-2018–184] and (3) the GEOCANTABRICAE research group, supported by the Asturian Regional Government (Spain) [grant number SV-PA-21-AYUD/2021/5176].

References

Álvarez-Marrón J, Hetzel R, Niedermann S, Menéndez R, Marquínez J (2008) Origin, structure and exposure history of a wave-cut platform more than 1 Ma in age at the coast of northern Spain: A multiple cosmogenic nuclide approach. Geomorphology 3–4:316–334. https://doi.org/10.1016/j.geomorph.2007.03.005

Anfuso G, Domínguez L, Gracia FJ (2007) Short and medium-term evolution of a coastal sector in Cadiz, SW Spain. Catena 2:229–242. https://doi.org/10.1016/j.catena.2006.09.002

Ballantyne CK, Dawson S, Dick R, Fabel D, Kralikaite E, Milne F, Sandeman GF, Xu S (2018) The coastal landslides of Shetland. Scott Geogr J 134(1–2):71–96. https://doi.org/10.1080/14702541.2018.1457169

Ballesteros D, Rodríguez-Rodríguez L, González-Lemos S, Giralt S, Álvarez-Lao DJ, Adrados L, Jiménez-Sánchez M (2017) New evidence of sea-level lowstands and paleoenvironment during MIS 6 and 4 in the Cantabrian coastal karst: the Cobiheru cave (North Iberia). Earth Surf Proc Land 42(11):1704–1716. https://doi.org/10.1002/esp.4115

Bieniawski ZT (1989) Engineering Rock Mass Classifications: A Complete Manual for Engineers and Geologists in Mining, Civil and Petroleum Engineering. Wiley, New York

Bird E (2000) Coastal Geomorphology: An Introduction. Wiley, New York

Bon de Sousa L, Loureiro C, Ferreira O (2018) Morphological and economic impacts of rising sea levels on cliff-backed platform beaches in southern Portugal. Appl Geogr 99:31–43. https://doi.org/10.1016/J.APGEOG.2018.07.023

Braathen A, HaraldBlikra L, Berg SS, Karlsen F (2004) Rock slope failures of Norway: type, geometry, deformation mechanisms and stability. Nor Geol Tidsskr 84(1):67–88

Camino Mayor J (1995) Los castros marítimos en Asturias. RIDEA, Oviedo

Church JA, Clark PU, Cazenave A, Gregory JM, Jevrejeva S, Levermann A, Merrifield MA, Milne GA, Nerem RS, Nunn PD, Payne AJ, Pfeffer WT, Stammer D, Unnikrishnan AS (2013) Sea Level Change. In: Stocker TF, Qin D, Plattner, G-K, Tignor M, Allen SK, Boschung J, Nauels A, Xia Y, Bex V, Midgley PM (eds.) Climate Change 2013: The Physical Science Basis. Contribution of Working Group I to the Fifth Assessment Report of the Intergovernmental Panel on Climate Change. Cambridge University Press, Cambridge, United Kingdom and New York. https://doi.org/10.1017/CBO9781107415324.026

Codrón JCG, Rasilla Álvarez DF (2006) Coastline retreat, sea level variability and atmospheric circulation in Cantabria (Northern Spain). J Coast Res 49–54. http://www.jstor.org/stable/25737381

De Lange WP, Moon VG (2005) Estimating long-term cliff recession rates from shore platform widths. Eng Geol 80:292–301. https://doi.org/10.1016/J.ENGGEO.2005.06.004

De Pippo T, Donadio C, Pennetta M, Terlizzi PC, F, Valente A, (2008) Coastal hazard assessment and mapping in Northern Campania, Italy. Geomorphology 3–4:451–466. https://doi.org/10.1016/j.geomorph.2007.08.015

Davidson-Arnott RGD (2010) Introduction to Coastal Processes and Geomorphology. University Press, Cambridge

Del Río L, Gracia FJ (2009) Erosion risk assessment of active coastal cliffs in temperate environments. Geomorphology 112(1–2):82–95. https://doi.org/10.1016/j.geomorph.2009.05.009

Domínguez-Cuesta MJ, Jiménez-Sánchez M, González-Fernández JA, Quintana L, Flor G, Flor-Blanco G (2015) GIS as a tool to detect flat erosional surfaces in coastal areas: A case study in North Spain. Geol Acta 13(2):97–106. https://doi.org/10.1344/GeologicaActa2015.13.2.2

Domínguez-Cuesta MJ, Ferrer Serrano A, Rodríguez-Rodríguez L, López-Fernández C, Jiménez-Sánchez M (2020a) Analysis of the Cantabrian Coast retreat around the Peñas Cape (Asturias, N Spain). Geogaceta 68:63–66

Domínguez-Cuesta MJ, González-Pumariega P, Valenzuela P, López-Fernández C, Herrera F, Mora M, Meléndez M, Marigil M.A., Espadas C, Cuervas-Mons J, Pando L, Jiménez-Sánchez M (2020b) The fast evolution of the Tazones Lighthouse landslide (N Spain): multidisciplinary 3D monitoring between 2018 and 2019. Geophys Res Abstr EGU2020b-10175. https://doi.org/10.5194/egusphere-egu2020-10175

Donelan MA, Drennan WM, Magnusson AK (1996) Nonstationary analysis of the directional properties of propagating waves. J Phys Oceanogr 26(9):1901–1914. https://doi.org/10.1175/1520-0485(1996)026%3c1901:NAOTDP%3e2.0.CO;2

Dufresne JL, Foujols MA, Denvil S et al (2013) Climate change projections using the IPSL-CM5 Earth System Model: from CMIP3 to CMIP5. Clim Dyn 40:2123–2165. https://doi.org/10.1007/s00382-012-1636-1

Duperret A, Genter A, Martinez A, Mortimore RN (2004) Coastal chalk cliff instability. In: NW France: role of lithology, fracture pattern and rainfall. Geol Soc Lond Eng Geol Spec Publ 20:33–55. https://doi.org/10.1144/GSL.ENG.2004.020.01.03

Duperret A, Rory NST, Martin Daigneault M (2005) Effect of groundwater and sea weathering cycles on the strength of chalk rock from unstable coastal cliffs of NW France. Eng Geol 78(3–4):321–343. https://doi.org/10.1016/j.enggeo.2005.01.004

Epifânio B, Zêzere JL, Neves M (2014) Susceptibility assessment to different types of landslides in the coastal cliffs of Lourinhã (Central Portugal). J Sea Res 93:150–159. https://doi.org/10.1016/j.seares.2014.04.006

Flor G, Busto JA, Flor-Blanco G (2006) Morphological and sedimentary patterns of ports of the Asturian Region (NW Spain). J Coast Res 48:35–40. https://www.jstor.org/stable/25737379

Flor G, Flor-Blanco G (2014) Raised beaches in the Cantabrian Coast. In: Gutiérrez F, Gutiérrez M (eds) Landscapes and Landforms in Spain. Springer, New York, pp 239–248

Flor-Blanco G, Flor G, Pando L, Abanades J (2015) Morphodynamics, sedimentary and anthropogenic influences in the San Vicente de la Barquera estuary (North coast of Spain). Geol Acta 13(4):279–295. https://doi.org/10.1344/GeologicaActa2015.13.4.2

Flor-Blanco G, Rubio-Melendi D, Flor G, Fernández-Álvarez JP, Jackson DWT (2016) Holocene evolution of the Xagó dune field (Asturias, NW Spain) reconstructed by means of morphological mapping and ground penetrating radar surveys. Geo-Mar Lett 36:35–50. https://doi.org/10.1007/s00367-015-0427-1

Flor G, Flor-Blanco G (2005) An Introduction to the Erosion and Sedimentation Problems in the Coastal Regions of Asturias and Cantabria (NW Spain) and its implications on environmental management. J Coast Res 49:58–63. http://www.jstor.org/stable/25737405

Gerivani H, Savari S (2019) Influence of wave force direction on cliff profiles: formulation and observation in a case of horizontally layered cliffs in the northern coast of Gulf of Oman. Arab J Geosci 12:498. https://doi.org/10.1007/s12517-019-4662-z

Griggs GB, Trenhaile AS (1994) Coastal Cliffs and Platforms. In: Carter RWG, Woodroffe CD (eds) Coastal Evolution: Late Quaternary Shoreline Morphodynamics. Cambridge University Press, Cambridge, pp 425–450

Gutierrez-Marco JC, Aramburu C, Arbizu M, Bernardez E, Hacar Rodriguez MP, Mendez-Bedia I, Montesinos Lopez R, Rabano I, Truyols J, Villas E (1999) Revision bioestratigrafica de las pizarras del Ordovicico Medio en el noroeste de Espana (zonas Cantabrica, Asturoccidental-leonesa y Centroiberica septentrional). Acta Geol Hisp 34(1):3–87. http://hdl.handle.net/10261/5226

Iannucci R, Martino S, Martorelli FN, Falconi L, Verrubbi V (2017) Susceptibility to Sea Cliff Failures at Cala Rossa Bay in Favignana Island (Italy). In: Mikoš M, Casagli N, Yin Y, Sassa K (eds) Advancing Culture of Living with Landslides. Springer, Cham. https://doi.org/10.1007/978-3-319-53485-5_63

ISRM (1981) Rock characterization testing and monitoring. ISRM suggested methods. Pergamon Press, Oxford

Izaguirre C, Méndez FJ, Menéndez M, Losada IJ (2011) Global extreme wave height variability based on satellite data. Geophys Res Lett 38:L10607. https://doi.org/10.1029/2011GL047302

Janeras M, Jara JA, López F, Marturià J, Royán MJ, Vilaplana JM, Aguasca A, Fàbregas X, Cabranes F, Gili JA (2015) Using several monitoring techniques to measure the rock mass deformation in the Montserrat Massif. In: IOP Conference Series: Earth and Environmental Science. https://doi.org/10.1088/1755-1315/26/1/012030

Jiménez-Sánchez M, Bischoff JL, Stoll H, Aranburu A (2006) A geochronological approach for cave evolution in the Cantabrian Coast (Pindal Cave, NW Spain). Z Geomorphol Supplementband 147:129–141

Jiménez-Sánchez M, Ballesteros D (2017) Metodología de evaluación del riesgo geoarqueológico en castros marítimos: El Castiellu (Asturias, España). Geogaceta 62:59–62. http://hdl.handle.net/10272/15174

Katz O, Reichenbach P, Guzzetti F (2011) Rockfall hazard along the railway corridor to Jerusalem, Israel, in the Soreq and Refaim valleys. Nat Hazards 56:649–665. https://doi.org/10.1007/s11069-010-9580-z

Kennedy DM, Coombes MA, Mottershead DN (2017) The temporal and spatial scales of rocky coast geomorphology: a commentary. Earth Surf Proc Land 42:1597–1600. https://doi.org/10.1002/esp.4150

Komar PD (1998) Beach Processes and Sedimentation, 2nd edn. Prentice-Hall, Englewood-Cliffs

Kopp RE, Horton RM, Little CM, Mitrovica JX, Oppenheimer M, Rasmussen DJ, Strauss BH, Tebaldi C (2014) Probabilistic 21st and 22nd century sea-level projections at a global network of tide-gauge sites. Earth's Future 2:383–406. https://doi.org/10.1002/2014EF000239

Lague D, Brodu N, Leroux J (2013) Accurate 3D comparison of complex topography with terrestrial laser scanner: Application to the Rangitikei canyon (N-Z). J Photogramm Remote Sens 82:10–26. https://doi.org/10.1016/j.isprsjprs.2013.04.009

Lateh H, Jefriza J, Rauste Y (2011) Monitoring slope based on SAR-interferometric technique and ground measurement. In: International Conference on Environment Science and Engineering, Bali, pp 188–191

Lauzon R, Murray AB, Cheng S, Liu J, Ells KD, Lazarus ED (2019) Correlation between shoreline change and planform curvature on wave-dominated, sandy coasts. J Geophys Res Earth Surf 124:3090–3106. https://doi.org/10.1029/2019JF005043

Le Bars E, Drijfhout S, De Vries H (2017) A high-end sea level rise probabilistic projection including rapid Antarctic ice sheet mass loss. Environ Res Lett 12(4):044013. https://doi.org/10.1088/1748-9326/aa6512

Lim M, Rosser N, Allison R, Petley D (2010) Erosional processes in the hard rock coastal cliffs at Staithes, North Yorkshire. Geomorphology 114:(1–2)12–21. https://doi.org/10.1016/j.geomorph.2009.02.011

Limber PW, Murray AB (2011) Beach and sea-cliff dynamics as a driver of long-term rocky coastline evolution and stability. Geology 39(12):1147–1150. https://doi.org/10.1130/G32315.1

López-Fernández C, Llana-Fúnez S, Fernández-Viejo G, Domínguez-Cuesta MJ, Díaz-Díaz LM (2020) Comprehensive characterization of elevated coastal platforms in the north Iberian margin: A new template to quantify uplift rates and tectonic patterns. Geomorphology 364:107242. https://doi.org/10.1016/j.geomorph.2020.107242

Marcos, A (1973) Las series del Paleozoico inferior y la estructura herciniana del occidente de Asturias (NW de España). Trabajos Geol 6:1–113. https://doi.org/10.17811/tdg.6.1973.3-113

Marqués FMSF (2006) Rates, patterns, timing and magnitude-frequency of cliff retreat phenomena A case study on the west coast of Portugal. Z Geomorphol Suppl Issues 144:231–257

Masselink G, Hughes MG (2003) Management of Coastal Erosion. In: Masselink G, Hughes MG (eds) Introduction to Coastal Processes & Geomorphology. Arnold, London, pp 1–307

Moñino M, Díaz de Terán JR, Cendrero A (1988) Pleistocene sea level changes in the Cantabrian coast Spain. In: Singh S, Tiwari RC (eds) Geomorphology and Environmental Management Allahabad Geogr. Soc., Allahabad, India, pp 351–364

Mora MA, Domínguez-Cuesta MJ, Jiménez-Sánchez M, López-Fernández C, Pando L, Meléndez M, Flor G, Marigil MA, Valenzuela P, Ballesteros D, Rodríguez-Rodríguez L (2018) Proyecto COSINES: abordando el reto de relacionar fenómenos meteorológicos costeros y retroceso de acantilados en Asturias. Acta J C Asoc Met Esp 35:169–171. https://doi.org/10.30859/ameJrCn35

Mortimore RN, Stone KJ, Lawrence J, Duperret A (2008) Chalk physical properties and cliff instability. Geol Soc Lond Eng Geol Spec Publ 20(1):75–88. https://doi.org/10.1144/GSL.ENG.2004.020.01.05

Moses C, Robinson D (2011) Chalk coast dynamics: Implications for understanding rock coast evolution. Earth-Sci Rev 3–4:63–73. https://doi.org/10.1016/j.earscirev.2011.08.003

Moura D, Albardeiro L, Veiga-Pires C, Boski T, Tigano E (2006) Morphological features and processes in the central Algarve rocky coast (South Portugal). Geomorphology 81(3–4):345–360. https://doi.org/10.1016/j.geomorph.2006.04.014

Neves M (2008) Anthropogenic modifications in the erosional rhythm of a coastal cliff. Rocha do Gronho (western coast of Portugal). J Iberian Geol 34(2):299–312. https://revistas.ucm.es/index.php/JIGE/article/view/JIGE0808220299A

Nicholls RJ, Cazenave A (2010) Sea-Level Rise and Its Impact on Coastal Zones. Science 328:1517–1520. https://doi.org/10.1126/science.1185782

Nicholls RJ, Lincke D, Hinkel J, Brown S, Vafeidis AT, Meyssignac B, Hanson SE, Merkens JL, Fang J (2021) A global analysis of subsidence, relative sea-level change and coastal flood exposure. Nat Clim Chang 11:338–342. https://doi.org/10.1038/s41558-021-00993-z

Noël T, Loukos H, Defrance D, Vrac M, Levavasseur G (2021) A high-resolution downscaled CMIP5 projections dataset of essential surface climate variables over the globe coherent with the ERA5 reanalysis for climate change impact assessments. Data Brief 35:106900. https://doi.org/10.1016/j.dib.2021.106900

Nunes M, Ferreira Ó, Loureiro C, Baily B (2011) Beach and Cliff Retreat Induced by Storm Groups at Forte Novo, Algarve (Portugal). J Coast Res 795–799. http://www.jstor.org/stable/26482281

Pérez-Alberti A, Pires A, Freitas L, Helder C (2013) Shoreline change mapping along the coast of Galicia, Spain. In: Proceedings of the Institution of Civil Engineers - Maritime Engineering 166(3):125–144. https://doi.org/10.1680/maen.2012.23

Prémaillon M, Regard V, Dewez TJB, Auda Y (2018) GlobR2C2 (Global Recession Rates of Coastal Cliffs): a global relational database to investigate coastal rocky cliff erosion rate variations. Earth Surf Dynam 6:651–668. https://doi.org/10.5194/esurf-6-651-2018

Ranasinghe R (2016) Assessing climate change impacts on open sandy coasts: A review. Earth Sci Rev 160:320–332. https://doi.org/10.1016/j.earscirev.2016.07.011

Salvini R, Francioni M, Riccucci S, Bonciani F, Callegari I (2013) Photogrammetry and laser scanning for analyzing slope stability and rockfall runout along the Domodossola-Iselle railway, the Italian Alps. Geomorphology 185:110–122. https://doi.org/10.1016/j.geomorph.2012.12.020

SanjoséBlasco JJ, Gómez-Lende M, Sánchez-Fernández M, Serrano-Cañadas E (2018) Monitoring Retreat of Coastal Sandy Systems Using Geomatics Techniques: Somo Beach (Cantabrian Coast, Spain, 1875–2017). Remote Sens 10(9):1500. https://doi.org/10.3390/rs10091500

SanjoséBlasco JJ, Serrano-Cañadas E, Sánchez-Fernández M, Gómez-Lende M, Redweik P (2020) Application of Multiple Geomatic Techniques for Coastline Retreat Analysis: The Case of Gerra Beach (Cantabrian Coast, Spain). Remote Sensing 12(21):3669. https://doi.org/10.3390/rs12213669

Scardino G, Sabatier F, Scicchitano G, Piscitelli A, Milella M, Vecchio A, Anzidei M, Mastronuzzi G (2020) Sea-level rise and shoreline changes along an open sandy coast: Case study of Gulf of Taranto, Italy. Water 12:1414. https://doi.org/10.3390/w12051414

Slangen AB, Katsman CA, van de Wal RS, Vermeersen LL, Riva RE (2012) Towards regional projections of twenty-first century sea-level change based on IPCC SRES scenarios. Clim Dyn 38:1191–1209 https://doi.org/10.1007/s00382-011-1057-6

Summerfield MA (1991) Global Geomorphology: An Introduction to the Study of Landforms Pearson. Prentice Hall England

Sunamura T (1983) A predictive model for shoreline changes on natural beaches caused by storm and post-storm waves. Trans Jpn Geomorphol Union 4–1:1–10

Sunamura T (1992) Geomorphology of rocky coasts. J Wiley, New York

Swirad ZM, Rosser NJ, Brain MJ, Vann Jones EC (2016) What controls the Geometry of Rocky Coasts at the Local Scale? J Coast Res 75:612–616 https://doi.org/10.2112/SI75-1231

Swirad ZM, Young AP (2021) Automating coastal cliff erosion measurements from large-area LiDAR datasets in California USA. Geomorphology 389:107799. https://doi.org/10.1016/jgeomorph2021107799

Tanabe A, Fukumizu K, Oba S, Takenouchi T, Ishii S (2007) Parameter estimation for von Mises-Fisher distributions. Comput Stat 22:145–157. https://doi.org/10.1007/s00180-007-0030-7

Terefenko P, Terefenko O (2014) Determining the role of exposure wave force and rock chemical resistance in marine notch development. J Coast Res 70(10070):706–711. https://doi.org/10.2112/SI70-105a1

Thiele ST, Grose L, Samsu A, Micklethwaite S, Vollgger SA, Cruden AR (2017) Rapid semi-automatic fracture and contact mapping for point clouds images and geophysical data. Solid Earth 8:1241–1253. https://doi.org/10.5194/se-8-1241-2017202017

Trenhaile AS (1987) The geomorphology of rock coasts. Clarendon Press, Oxford

Trenhaile AS (1989) Sea level oscillations and the development of rock coasts. In: Lakhan VC, Trenhaile AS (eds.) Applications in Coastal Modeling, Elsevier, Amsterdam, pp. 271–295. https://doi.org/10.1016/S0422-9894(08)70129-6

Trenhaile AS (2002) Modelling the development of sloping marine terraces on tectonically mobile rock coasts. Mar Geol 185:341–361. https://doi.org/10.1016/S0025-3227(02)00187-1

Trenhaile AS (2016) Rocky coasts — their role as depositional environments. Earth-Sci Rev 159:1–13. https://doi.org/10.1016/jearscirev201605001

Trenhaile AS, Kanyaya J (2007) The Role of Wave Erosion on Sloping and Horizontal Shore Platforms in Macro- and Mesotidal Environments. J Coast Res 23(2)298–309. http://www.jstororg/stable/4494200

Tsujimoto H (1987) Dynamic conditions for shore platform initiation. Science Report of the Institute of Geoscience, University of Tsukuba (Japan) A 8, pp 45– 93

Wangensteen B, Eiken T, Odegard RS, Sollid JL (2007) Measuring coastal cliff retreat in the Kongsfjorden area, Svalbard, using terrestrial photogrammetry. Polar Res 26:14–21

Wolters G, Müller G (2004) The propagation of wave impact induced pressures into cracks and fissures. Geol Soc Lond Eng Geol Spec Publ 20:121–130. https://doi.org/10.1144/GSLENG20040200109

Young AP, Guza RT, Flick RE, O'Reilly WC, Gutierrez R (2009) Rain waves and short-term evolution of composite sea cliffs in southern California. Mar Geol 267:1–7. https://doi.org/10.1016/jmargeo200908008

Young AP, Carilli JE (2019) Global distribution of coastal cliffs. Earth Surf Process Landforms 44:1309–1316. https://doi.org/10.1002/esp4574